Electronic Supplementary Information (ESI)

Multiple Reaction Monitoring (MRM)-Profiling with Biomarker Identification by LC-QTOF to Characterize Coronary Artery Disease

Karen E. Yannell[1], Christina R. Ferreira[1], Shane Tichy[2], R. Graham Cooks[1]

[1] Chemistry Department, Purdue University, West Lafayette, IN 47907, US

[2]Agilent Technologies, Santa Clara, CA 95051, US

Table of Contents

1. EXPERIMENTAL SYSTEM

1.1 Instrument Configuration and Sample Introduction

Multiple reaction monitoring (MRM)-profiling is faster than liquid chromatography mass spectrometry (LC-MS) metabolomics methods because it directly introduces a diluted sample or simple extract into the MS. No time or materials for chromatography are required. Instead, with direct infusion (DI) or flow injection (FI) techniques, in lieu of LC, the user saves time and resources and they also analyze an intact or near intact sample. Ideally, no complex sample pretreatment is needed, just a simple dilution or fast extraction. Therefore, DI or FI can measure many analytes with varying chemical properties.[1, 18] This is a move closer to universal analysis of the metabolome.[1, 2]

FI is automatic and carries a small volume of diluted sample or extract (20 -40 µL plug of sample) to the electrospray ionization source through LC pump lines with the solvent flow. However, as seen with this coronary artery disease (CAD) method and elsewhere, it can be more time consuming since the sample must travel to the source and more time is required for cleaning the solvent lines.[35] DI methods continuously introduce sample into the MS. These methods may require a larger volume of diluted sample (>200 µL) and are difficult to automated. However, they are much faster since they require nearly no time to reach the source and minimal cleaning.

Another methodology that could be used with MRM-profiling is nano-infusion.[1, 2] This is similar to DI but it uses a very small amount of sample 5-20 µL diluted sample and requires no time for cleaning since the nozzles are single use. This has been automated and is therefore amenable to high throughput analysis.[1] However, the method is sensitive to high salt content so not every biological sample may work with this setup. Ambient ionization methods may also be used but have been developed minimally with MRM-profiling. Briefly, paper spray ionization is limited by the time it can spray the sample, can have high background noise, and, similar to chromatography, some analytes can be retained on the paper and not analyzed.[12]

If methods need to be faster and without a discrimination study to minimize the transition set, DI and nano-infusion methods should be used. DI and nano-infusion methods continuously introduce sample to the MS, have less chance of carryover, and in principle should be faster than FI. As demonstrated with this method, FI methods have a discrete amount of time the sample is introduced and may require more than one injection to collect data for all the ion transitions. Each injection takes time to travel to the source and requires additional time to clean solvent lines. This adds significant time to the method and a discrimination study is performed to reduce the analysis time.

1.2 Sample Preparation

For high throughput sample preparation, several of these steps were automated by using a Bravo liquid-liquid handler (Table S1) and 96-well plates were employed. Given more time for development the whole workflow could be automated.

Table S1 Modified Bligh-Dyer sample preparation procedures of human plasma for MRM-profiling [a]

Step:	Addition of:	Volume (µL)	Manual/Bravo
1	Plasma	40	Manual
2	Chloroform	100	Bravo
3	Methanol	180	Bravo
4	Vortex, 30s		Manual
5	Chloroform	100	Bravo
6	Water	100	Bravo
7	Vortex, 60 s		Manual
8	Centrifuge, 60 m, 4000 RPM		Manual
9	Collect 75 µL top and bottom layer, place in new container		Manual

10	Dry down, SpeedVac, 50C, ~3hr		Manual
11	Solvent	300	Bravo
12	Sonicate, 10 m		Manual
13	Centrifuge, 10 m, 4000 RPM		Manual
14	Dilute 20X into solvent		Bravo

a) The addition of samples and reagents and their respective volumes are listed. Notes for if the step was performed manually or by the Bravo liquid-liquid handler and additional sample preparation details are given.

After step 8, of sample preparation (Table S1) three layers exist, a top aqueous and polar layer containing polar metabolites, a middle solid white layer of protein, and a bottom chloroform layer containing lipids. An issue that arose during the project was that the protein layer did not fully pack and would inconsistently interfered with the collection of the lower layer. More centrifugation was needed for these samples. This could be avoided in future experiments by (1) using less plasma and thus minimizing the protein layer or (2) using a higher speed rotor for centrifugation (20,000 rpm, not 4,000 rpm). These suggestions were tested successfully on a single sample.

This final sample preparation procedure was used for every MRM-profiling experiment. During development, the sample preparation was often performed one sample at a time, not a 96 well plate format, or using alternative volumes. These differences are noted for each experiment in the sections below.

2. METHOD DEVELOPMENT

2.1 Solvent Evaluation

The solvent and modifier conditions are influential parameters for this analysis and their development should be considered for every MRM-profiling project. For MRM-profiling the solvent and source conditions should aim to dissolve and ionize all analytes in the sample. Given the diversity of the analytes in a biological system this is difficult to achieve. If information is known about the analytes in the sample or of interest in the disease, a solvent can be tailored for those. In no information about what analytes are of interest, then optimization should aim at detection of as many different types of analytes as possible. For the CAD solvent optimization, tradeoffs in ionizing one class of molecules over another occurred. But by exploring different options with simple experiments, clear data was gathered as to which solvent was best.

A few solvents were tested with the plasma extract. These were known to give good signal for lipids, however, their performance with small metabolites was unknown.[13, 36, 52] The following solvents were used both to reconstitute the dried plasma extracts (step 11, Table S1) and as the pump solvent.

1: 70% acetonitrile, 30% methanol, 10 ppm ammonium formate, 0.1% formic acid

2: 90% methanol, 10% chloroform, 10 ppm ammonium formate, 0.1% formic acid

3: 66% chloroform, 33% methanol, 10 ppm ammonium formate, 0.1% formic acid

2.2 Ion Source Conditions

Source conditions with the Agilent Jet Stream (AJS) needed to be optimized for each solvent system under consideration. This was done manually by optimizing the parameters in Table S2. The parameters were optimized in the order listed by injecting a reserpine standard diluted in the solvent and selecting the condition with the highest absolute signal intensity. Also, a phosphotidylcholine (PC) lipid was added to the sample to have optimization run including a lipid molecule. The AJS parameters for solvent 1 and solvent 2 are in Table S2.

Table S2 AJS source parameters optimized with the ranges and steps tested [a]

Parameter	Unit	Range	Step	Solvent 1	Solvent 2
Capillary voltage	V	2000-4000	500	2500	3500
Sheath gas temperature	C	50-300	50	150	200
Sheath gas flow	L/min	4-12	2	6	6
Gas temperature	C	50-350	50	300	350
Gas flow	L/min	3-13	2	7	11
Nebulizer	psi	20-60	10	25	60

a) Each parameter was tested individually by injecting a standard (n=3) and selecting the value with the highest MRM signal of the standard. AJS parameters optimized for solvent 1 and solvent 2 when using a flow rate of 0.05 mL/min are listed as well.

The nozzle voltage was not evaluated and this remained at 1500V for all experiments. These parameters were optimized using a flow rate of 0.05 mL/min. For any flow rate significantly different from this, source conditions may need to be reevaluated. Under these conditions, solvent 1 and 2 had pressures of 20 and 30 bar, respectively.

2.3 Data for Different Solvents and Collision Energies

Solvent 3 is commonly used for lipid analysis.[52] However, here it caused the ammonium formate to crash out in the source and continuously clogged the nebulizer regardless of the AJS source parameters. This solvent was therefore eliminated. With optimized AJS conditions, solvent 1 gave 100X greater signal for reserpine. Analysis of an undiluted plasma extract in solvent 1 gave very good results for a PC, positive mode, precursor (Prec) 184 scan (data not shown).

However, upon inspecting the negative mode, it was found that the solvent 1 did not dissolve and/or ionize the plasma extract sample well. Figure S1 shows negative mode full scan spectra of the lipid region, *m/z* 530-980. No negative mode peaks were seen with solvent 1 (Figure S1, A) but solvent 2 had distinct lipid signals (Figure S1, B). Solvent 2 was selected and evaluated for acid addition.

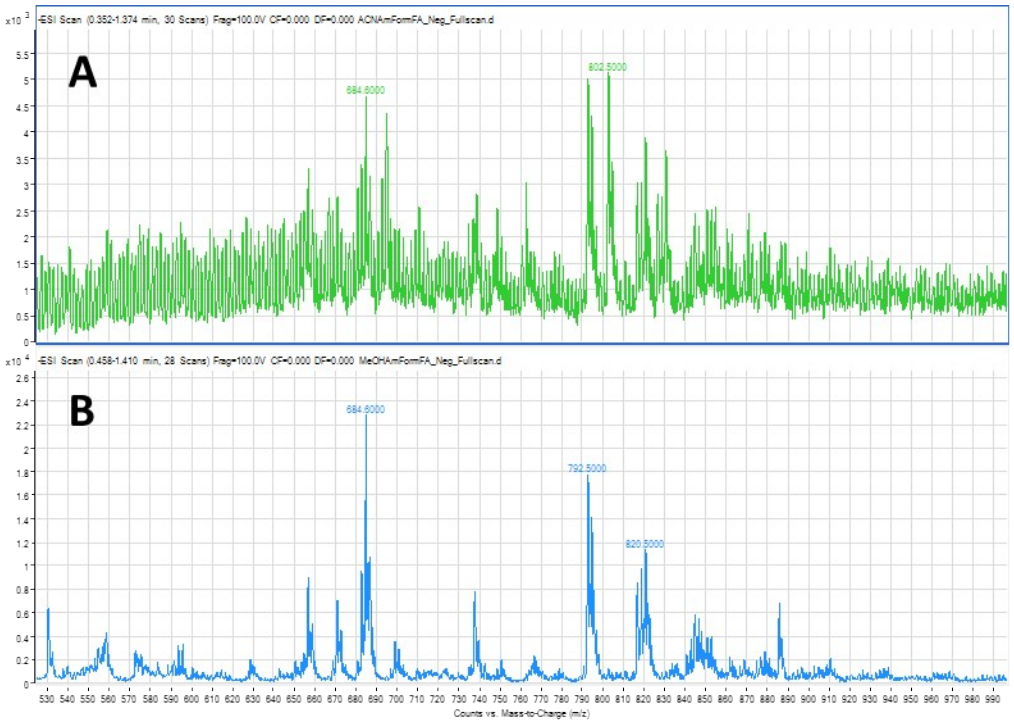

Figure S1 Negative mode, full scan spectra from *m/z* 530-990 of a human plasma extract reconstituted and injected with either (A) solvent 1 (70% acetonitrile, 30% methanol, 10 ppm ammonium formate, 0.1% formic acid, top) or (B) solvent 2 (90% methanol, 10% chloroform, 10 ppm ammonium formate, 0.1% formic acid, bottom).

Modifiers help create certain adducts but they should only be used if they do not impair compound ionization of other analytes. Figure S2 shows positive mode, Prec spectra of human plasma sample in solvent 2 prepared with (A) and without acid (B). The solvent with acid had 10^4 signal and many small metabolites below *m/z* 315 were only seen with this solvent. However, the peaks that appeared with no acid, namely *m/z* 369.1 and 426.0 were present at the same intensity in both solvents.

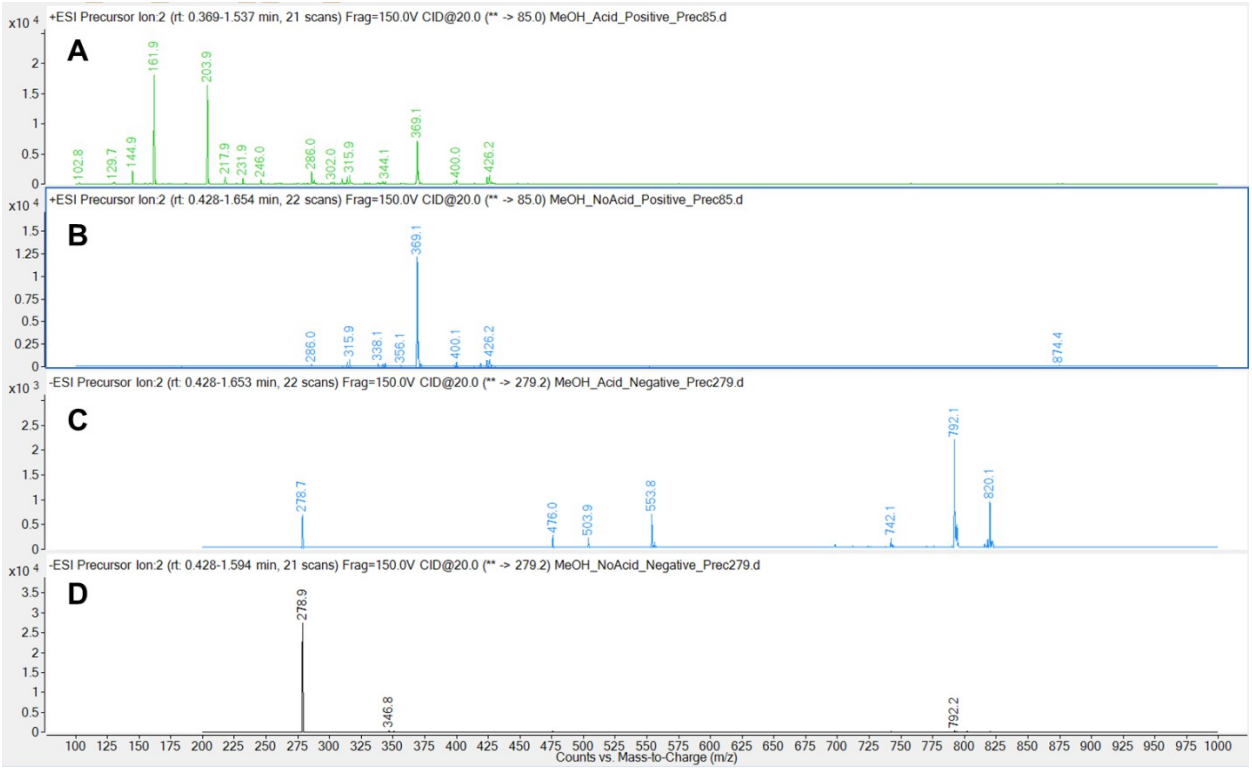

Figure S2 Positive mode, Prec 85 scan (CE 20) from *m/z* 100-1000 of plasma sample prepared and sprayed with solvent 2 with acid (A) and solvent without acid (B). Negative mode, Prec 279.2 scan (CE 20) from *m/z* 200-1000 of plasma sample prepared and sprayed with solvent 2 with acid (C) and solvent without acid (D).

Similar profiles are found for both solvents in the negative mode (Figure S2, C and D). A Prec 279.2 scan using solvent (C) which contains acid gave several additional peaks compared to solvent without acid (D). Because of the numerous additional peaks in both the positive and negative mode, the acidified solvent was better for this method than the solvent without modifier.

The use of the automated auto-sampler required a solvent for washing the needle that collected and injected the sample to prevent needle carryover. A 2:2:1 mixture of methanol: isopropyl alcohol: chloroform was selected to remove both polar and lipid material.

2.4 Precursor and Neutral Loss Scan Optimization

Initial Prec and neutral loss (NL) tests were performed using a pooled plasma sample prepared with solvent 1. Samples were treated as described in Table S1 except that 150 µL of the top and bottom layers were collected, the sample was dried for a longer period of time at 36 C, and the sample was reconstituted in 400 µL solvent 1. This sample was then tested with no further dilution and also with a 20X and 200X dilution of the reconstituted extract into solvent 1.

For optimization a random selection of Prec and NL scans in both positive and negative mode were selected to be used for optimization of scan parameters. The goal was to create a method that was fast, reproducible, required one injection of sample, measured three or more collisions energies, and could easily be analyzed with MassHunter Qualitative software. The dilutions of the sample extract were also tested and carryover initially evaluated. Note, all Prec and NL scans covered the largest mass/charge range possible from *m/z* 50-1000 but certain NL scans were limited on the low end. Discovery scans for some MRM-profiling projects could go higher than this range.

2.5 Precursor and Neutral Loss Optimization Data

Optimized scan speed and sample injection volume were key for obtaining good spectra in one injection for three CE values (5, 20, and 35 eV). Figures S3 and S4 show spectra collected at different scan speeds with a positive mode NL 32 and NL 299 scan, respectively. The NL 32 scan (Figure S3) is one that gives low single from this sample overall and it has the largest expected scan range of any of the scans in the discovery phase. If this scan can be improved it is assumed the data for all the other Prec and NL scans will also improve. The 200 ms scan speed (Figure S3, A) is too fast to measure any significant signal. The 500 and 1000 ms scans (Figure S3, B and C) show a higher *m/z* 126.9 peak but the 2000 ms scan (Figure S3, D) shows the highest intensity for *m/z* 126.9 and a clear *m/z* 318.9 peak.

The NL 299 scan in Figure 4S has a much higher signal overall from the human plasma extract. However, an improvement in peak shape can be seen in the *m/z* 820-920 region as scan time increases from 500 to 1000 ms (Figure S4 A, B). In both these examples, spectrum quality can be improved by increasing scan time and this parameter should always be evaluated for discovery phase experiments.

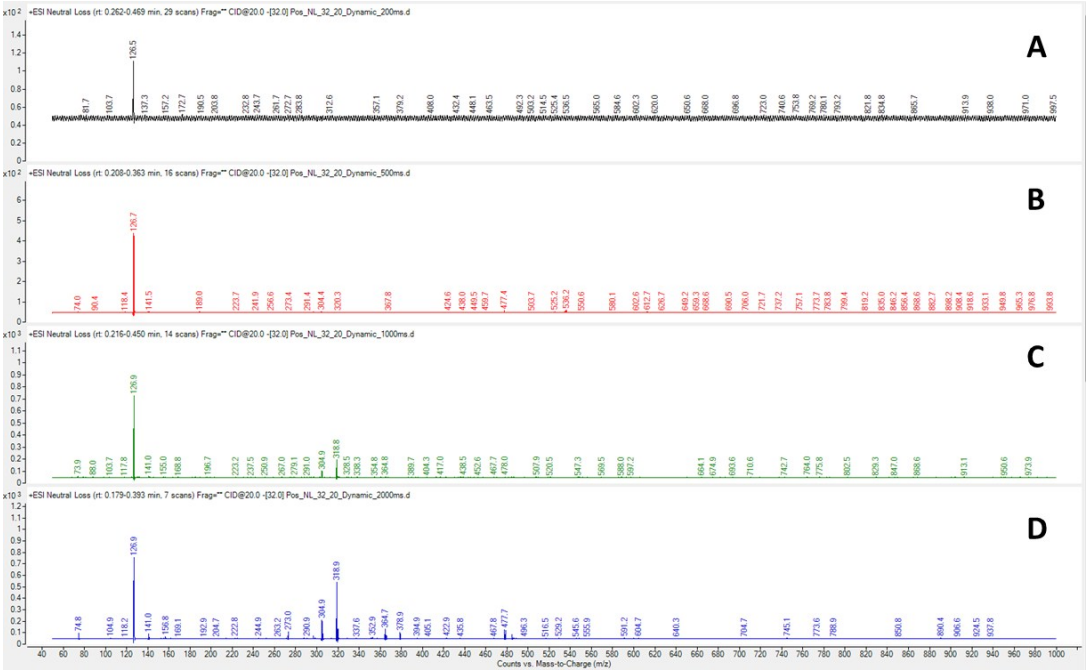

Figure S3 Positive mode NL 32 from *m/z* 50-1000 collected with four different scan times: 200 (A), 500 (B), 1000 (C), and 2000 (D) ms. This data was collected with a 200X diluted human plasma extract in solvent 2.

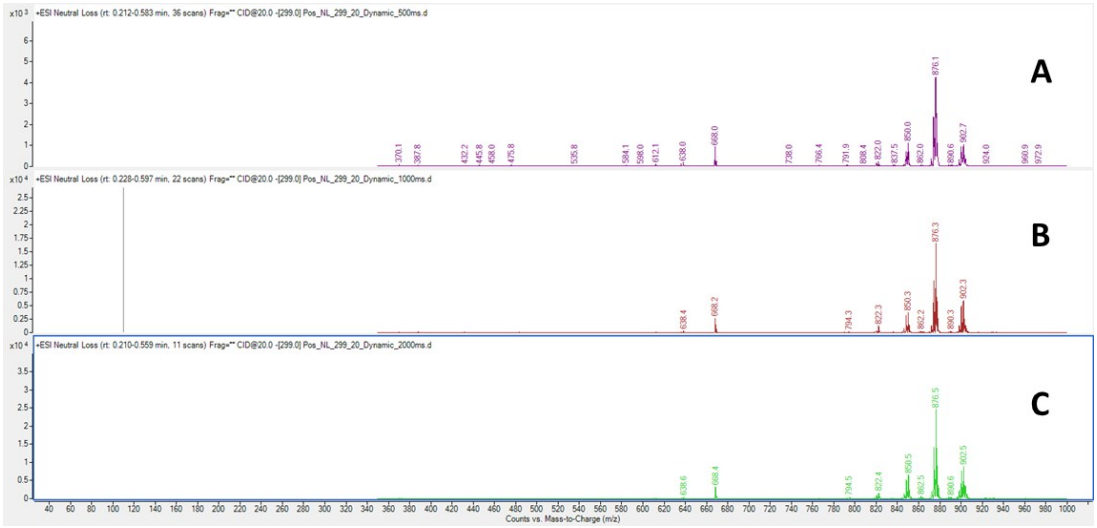

Figure S4 Positive mode NL 299 from *m/z* 350-1000 collected with three different scan times: 500 (A), 1000 (B), and 2000 (C) ms. This data was collected with a 200X diluted human plasma extract in solvent 2.

In order to collect enough scans at three different CE (5, 20, 35 eV; 5-10 scans/CE) with a 1000 or 2000 ms scan time the length of time sample is sprayed into the MS must be increased. This can be accomplished by slowing down the flow rate to below 0.05 mL/min or by injecting more than 20 µL of sample.

With the 1290 pump, the flow rate cannot be decreased without lowering the pressure to below 30 bar. Slowing down the flow rate was not an option with this configuration but it could be with a nanoLC. A better approach was to inject more sample. Given the sample preparation procedure, this is not an issue for plasma extracts but for projects with more precious sample this may not be possible and nano-infusion or DI might be a better option. Figure S5 shows a positive mode NL 299 scan injected with 20, 30, and 40 µL of a 20X dilution of plasma extract. There is a clear increase in the time the sample was sprayed for the larger injection volume. Using 80% absolute intensity (y-axis) as a marker for sample cutoff, it can be approximated the spray times for the 20, 30, and 40 µL injections are approximately 0.3, 0.5, and 0.9 minutes, respectively. The subsequent spectra show no difference in signal intensity or quality of peaks (Figure S5, inset). Note the tailing in the signal increases as the sample volume increases suggesting that a larger sample volume may require a longer wash period to prevent carryover.

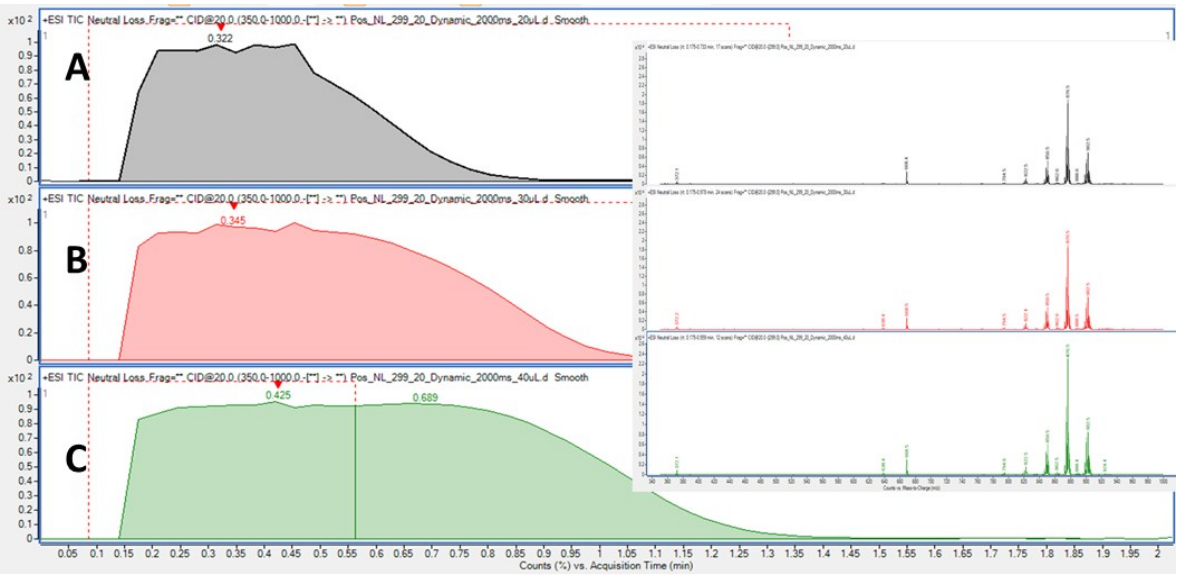

Figure S5 Three TICs of a plasma extract (20X dilution) injected at 20 (A), 30 (B), 40 (C) µL volumes. Extreme smoothing parameters were applied to get automatic integration. The spectra (inset) are averaged over the whole TIC integration.

With the larger injection volume it was possible to measure three CE in one injection and record ten scans using a 1000 ms scan speed (Figure S6). In order to simplify and automate data extraction, MassHunter Qualitative workflow was used. For each data file, the TICs for individual CE were separated. Next, the TIC signal could be smoothed into a pseudo Gaussian peak (as shown in Figure S5) and automatically integrated. Another approach was to alter the acquisition method to measure three different time segments. Segment one was full or product ion scan. Segment two was the Prec or NL scan for that method and it began when the sample is eluting. Segment three was a full or product ion scan and ended at the end of the injection (including the line wash). After the TIC for each CE was extracted, the extracted chronogram appears as a short segment of signal and was easily integrated (Figure S6). In all cases, a Qualitative software summation integration feature would benefit the Prec and NL scan data analysis workflow.

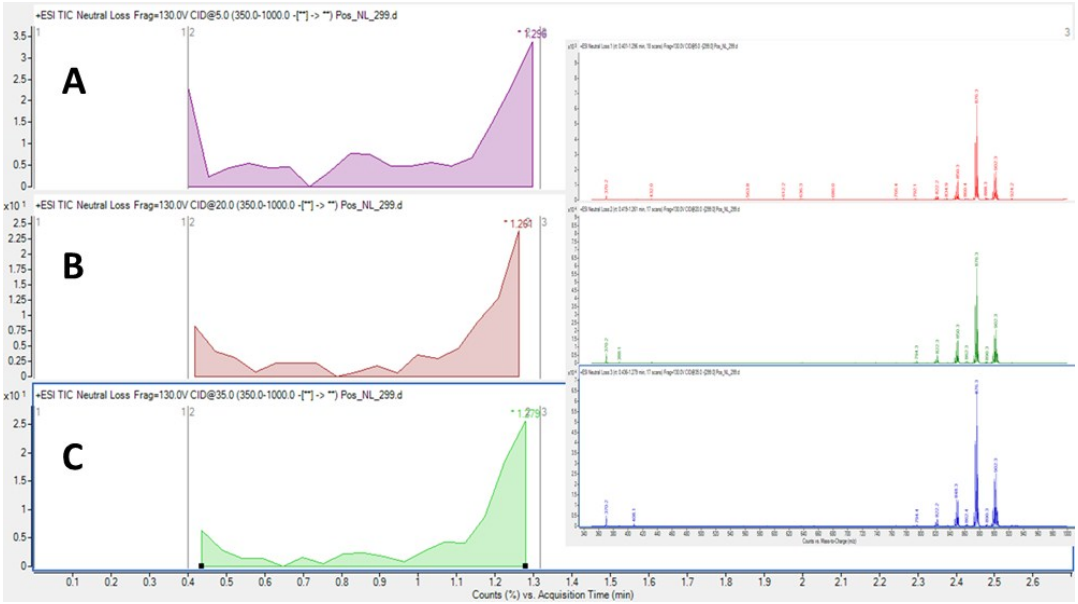

Figure S6 Positive mode NL 299 chronogram with three CE extracted and manually integrated. The data starts and stops at discrete points because the NL 299 scan was only set for that time segment. A, B, and C represent 5, 20, and 35 eV, respectively.

The 'Fragmentor Mode' in MassHunter Acquisition can be set to either 'Fixed' or 'Dynamic' mode. This was evaluated using two methods. One method was set to dynamic with a voltage ramp that include three ions: *m/z* 118.0 at 90V, *m/z* 666.5 at 130 V, and *m/z* 874.6 at 210 V. The other method had a fixed fragmentation energy of 130 V. Spectra collected with both methods were compared (Figure S7). The signal quality appeared to be better for the fixed methods (Figure S7, A and D) and so the fragmentor was fixed in the Prec and NL methods. This may change given a different mass range and should be evaluated if the mass range changes.

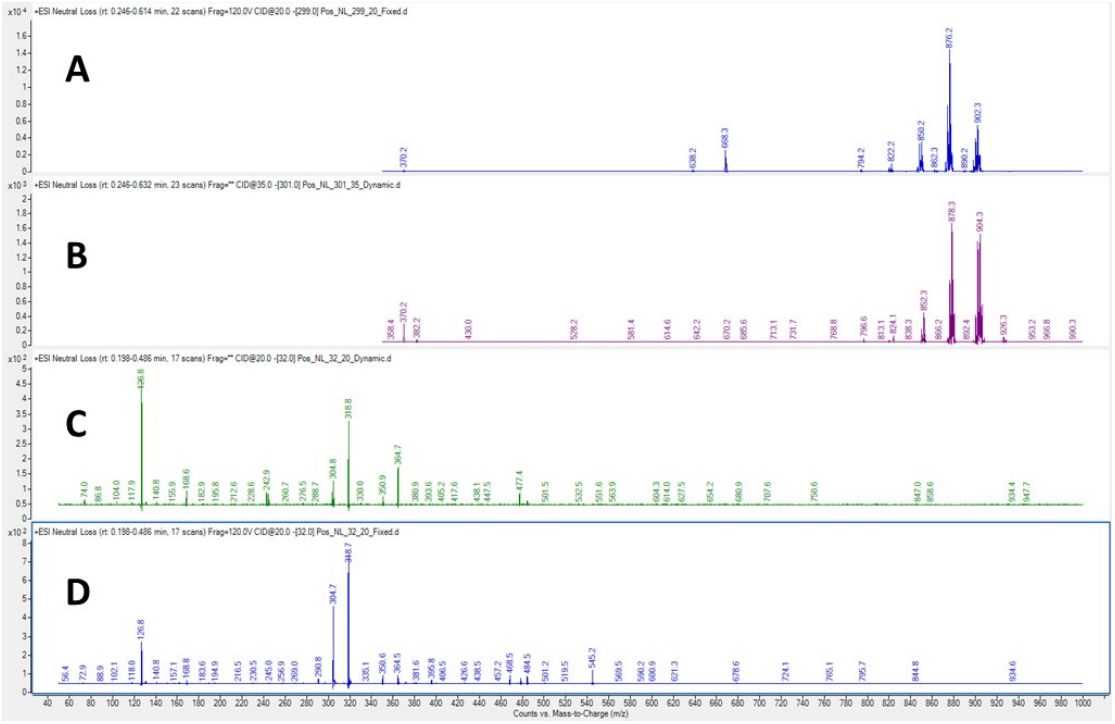

Figure S7 Fixed (A and D) and dynamic (B and C) fragmentor voltages for positive mode NL 301 scan (A and B) and positive mode scan (C and D). A 20X dilution of a plasma sample in solvent 2 was used for both.

One example of the final Prec and NL scan method is shown in Figure S8. Each Prec and NL scan had its own method. A full list of the Prec and NL scans is listed in the Table S5. These scans and their values were taken from literature sources and is continuously growing.[4, 37-46] Note not all Prec and NL scans need to be performed for every experiment. If *a priori* knowledge suggests targeting a group of molecules characterized by a few functional groups then those can be collected. However, if a project aims for independent (unsupervised) discovery, then many or all of the scans should be performed.

A

Time segments

#	Start Time	Scan Type	Div Valve	Delta EMV (+)	Delta EMV (-)	Stored
1	0	Product Ion	To MS	0	0	☑
▶ 2	0.4	Neutral Loss	To MS	0	200	☑
3	1.3	Product Ion	To MS	0	0	☑

B

Acquisition | Source | Chromatogram | Instrument | Diagnostics

Scan segments

Segment Name	Neutral Loss	MS1 From	MS1 To	Scan Time	Frag Mode	Fragmentor	Collision Energy	Cell Accelerator Voltage	Polarity
▶	121	150	1000	1000	Fixed	130	35	5	Negative
	121	150	1000	1000	Fixed	130	20	5	Negative
	121	150	1000	1000	Fixed	130	5	5	Negative

Figure S8 Example of MassHunter QQQ Acquisition method for Prec and NL scans. A) Time segments were used to measure the Prec or NL from 0.4 min to 1.3 min. B) An example of the acquisition parameters used for Prec and NL scans. The mass range was maximized in each scan by setting 'MS1 From' to the lowest possible value but 'MS1 To' never exceeded *m/z* 1000.

Carryover should be initially assessed at this point. Three blanks (solvent 2) were analyzed with representative scans. Then, six samples were analyzed followed by three more blanks. The needle wash time or the wash solvent can be changed to remove sample carryover from the well. Removing carryover in the lines with a longer wash period should be avoided because it increases the method time (injection to injection) and decreases throughput of the method. In all of the above experiments a 20X dilution provided high signal for various analytes, did not appear to have carryover, and was chosen as the sample preparation dilution at this stage.

For the discovery phase, each study should have a minimum of two pooled samples (*i.e.* control and disease). This pooling can be simple: mix ten disease and ten control samples to make a disease and control pool. Ideally there would be more than ten individual samples in each pool to reduce the variability even more. Additionally, more groupings can be created to emphasize different biomarkers related to subpopulations of a disease or different severities of disease. Subpopulation pools are good to include so their specific up regulated biomarkers will be higher and related transitions will therefore be included in the MRM method. This allows for variants of the analytical procedure to be performed after data collection. For this project, control, high CAD, low CAD and peripheral artery disease (PAD) pools were each created from 30 individual samples. The high and low designations were taken from descriptions in the clinician notes of the diagnosis (*i.e.* severe and mild).

To create list of transitions from the Prec and NL data, a MassHunter Qualitative workflow was used to work up each data file. First, chronograms were separated by CE, then integrated, *m/z* peak lists copied to Excel. In the Qualitative workflow a noise threshold was applied to the peak list (*i.e..* 500 counts). To make the transition lists (from the Prec or NL data), the following parameters for each *m/z* peak were listed in Excel: mode (positive or negative), precursor ion, scan type (Prec or NL), scan value (Prec or NL value), CE (eV), and intensity of the peak (counts). From the precursor ion *m/z* value*,* scan type, and scan value the product ion was calculated. After the signals for all the transitions were combined, there were overlapping transitions. Filtering was done to leave one unique transition per CE (parameters with the highest intensity were retained). Additional filtering was done to remove overlapping transitions *e.g.* 780.1→ 184.0 vs 780.2→184.0.

The final list of transitions discovered with Prec and NL scans vary in length (500-6000 transitions) depending on how many scans are tested, the *m/z* range of the scans, the complexity of the sample, and the criteria for 'discovery'. In summary, this Prec and NL experiment optimization aimed to create a scan method that acquired fast and reproducible signal. In the workflow, the data was easily extracted and combined in a final transition list for MRM experiments.

2.6 MRM Optimization

Many of the parameters optimized in Prec and NL development were carried over to the MRM method. The final parameter to optimize was dwell time. The sample preparation and total MRM method reproducibility were also evaluated at this stage.

The dwell time optimization study used a pooled sample prepared as described in Table S3 but with a 20X dilution. Methods with varying dwell times (5-100 ms) were created and each contained the thirty highest and thirty lowest responding transitions. The pooled sample was injected six times for each method. The height of each transition was recorded and the relative standard deviation (RSD) for the height was calculated (Table S3).

Table S3 Dwell time study summary [a]

30 Highest Intensity Transitions					
Dwell time (ms)	5	10	20	50	100
Average height (counts)	160,509	161,387	161,677	158,929	131,661
Average RSD	4%	3%	3%	3%	2%
RSD above 10%	0	0	0	0	0
30 Lowest Intensity Transitions					
Dwell time (ms)	5	10	20	50	100
Average height (counts)	768	757	736	723	703
Average RSD	9%	8%	6%	4%	4%
RSD above 20%	1*	0	0	0	0
RSD above 15%	3*	4*	0	0	0

a) MRM methods with different dwell times contained 60 transitions and were measured with a human plasma extract (20X dilution) 6 times. Average height of the transitions and RSD are listed. The number of transitions with RSDs above 10%, 15%, or 20% are reported. The * indicates that the transitions were below 200 counts.

The data showed that the highest responding transitions were very reproducible. All had RSDs below 10% and the average RSD for all the transitions was below 5%. The lowest responding transitions had more error as the dwell time decreased. The average RSD at 5 ms was 9% compared to 4% at 100 ms. However, this seemed to be caused by a few very poorly responding transitions (<200 counts). These transitions were likely noise and when they were removed the RSDs for all transitions and dwell times were below 15%. This data proves that a 5 ms dwell time is very reproducible with on the 6470 QQQ with these transitions and sample. This instrument can collect data even faster (0.5 ms dwell time). However, this is not necessary for our experiments due to a common software limitation; the MassHunter Acquisition software cannot contain more than 500 transitions per segment.

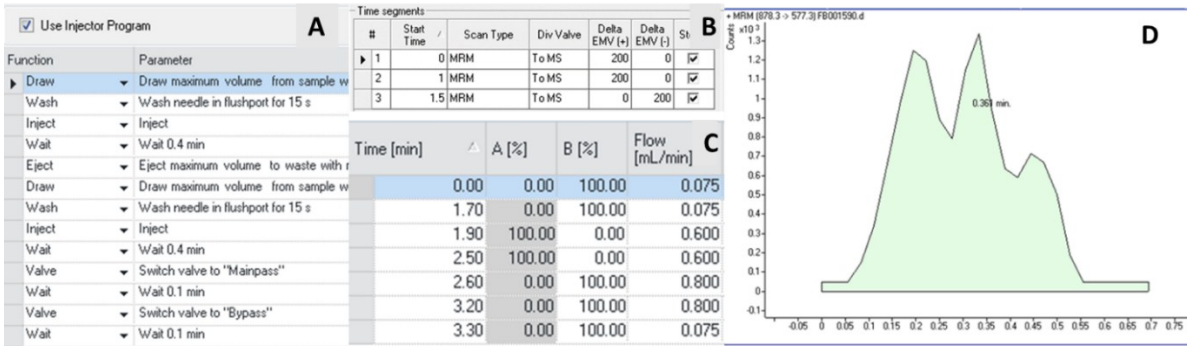

Figure S9 The final method utilized an injector program (A) to inject three 20 µL injections per data file. Each injection was analyzed with a different transitions set by defining time segments (B). The pump (C) ran at a 75 µL/min flow rate (Bottle B, solvent 2) followed by a wash method to clean the pump lines (Bottle A, 40% Methanol, 40% isopropyl alcohol, 20% chloroform). The data was integrated in MassHunter Quantitative software using spectral summation tool (D).

2.7 Evaluation of Performance

Until this point, sample preparation was performed on an individual sample scale. Testing the reproducibility of a 96-well plate sample preparation method is important to ensure each sample is prepared correctly by the procedure and liquid handler. This also tests the robustness of the FI-MRM method over many samples and a longer time period. For this study, a pooled sample was pipetted 96 times on a well plate and worked up using the method in Table S1 but with a 20X dilution. One injection per well was acquired using the MRM method. The principal component analysis (PCA) (Figure S10) showed separation of the samples over time. The first 48 injections (red) were separating from the last 48 injections (green).

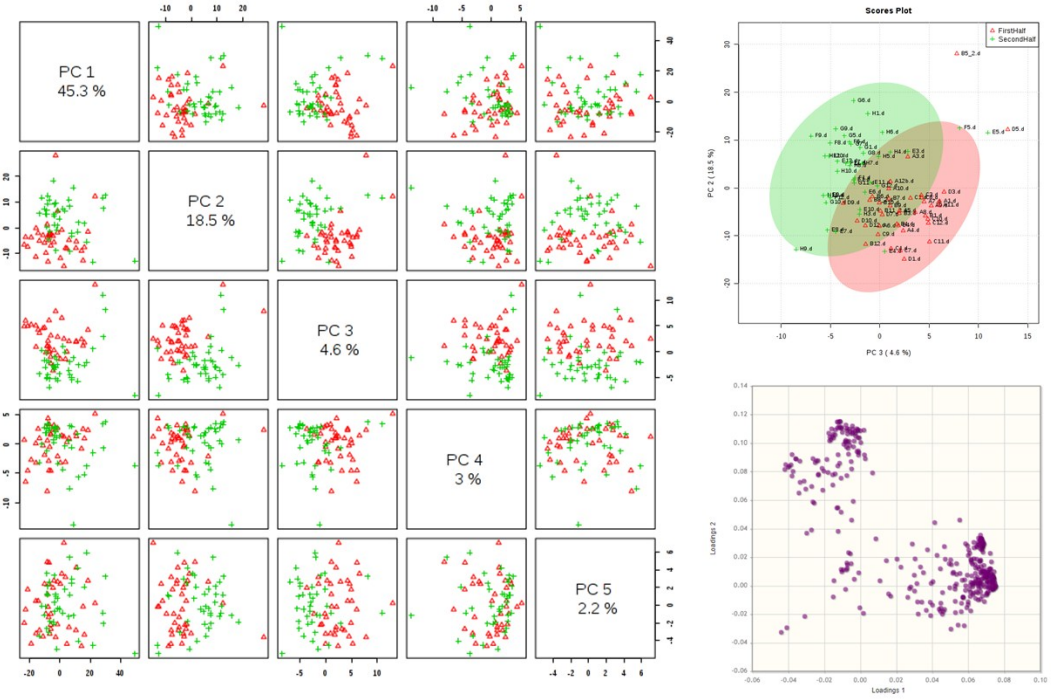

Figure S10 PCA plots for the first half (red) and second half (green) of a plate prepared with the same sample and collected using the same MRM method. The loading plot (bottom right) shows separation between identical lipid transitions due to carryover.

After investigating the issue, an increase in lipid signals was causing the separation (Figure S10, loading plot). This was due to carryover that was not detected previously. In an earlier study, carryover was evaluated by analyzing before and after solvent blanks with six injections of a 20X diluted sample in between. With Prec and NL scans, this showed no significant carryover. However, if 20 or more samples were injected, carryover was observed on the MRM method. The use of a quality control sample, which would be injected regularly between each few samples would detect this issue and make the bias quantifiable. It is hypothesized that lipids began to adhere to the stainless steel tubing and were subsequently observed in the after blanks. Initially, to solve this problem, a number of wash methods and solvents were tested to clean the lines after each injection. These did not work well enough and a dilution of the sample was ultimately made (200X verses 20X). The final method had a more thorough washing of the lines and a larger dilution (200X) to prevent carryover. The data from four plates of individual samples were not separating significantly and the method was therefore reproducible (Figure S11).

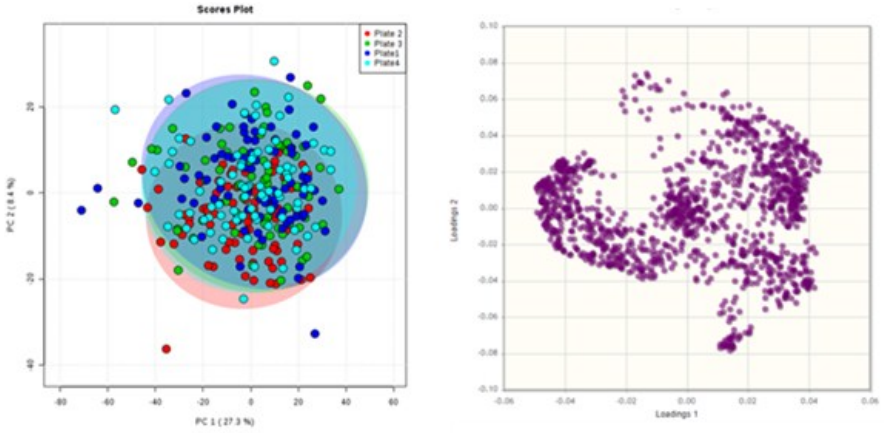

Figure S11 PCA plot of four 96-well plates of random samples with data and collected using the same MRM method. The loading plot does not show separation of any one or any group of analytes.

3. ANALYTE IDENTIFICATION BY LC-HRMS

3.1 LC-MS Methods

A ZORBAX Eclipse Plus RRHD C18, 2.1 × 150 mm, 1.8 µm column was used for separating the analytes. IPA/MeOH/water (5:1:4) with 5 mM ammonium acetate and 0.1 % acetic acid (Pump A) and IPA/water (99:1) with 5 mM ammonium acetate and 0.1 % acetic acid (Pump B) were used as mobile phases. The gradient and source conditions are reported in Figure S12. A 2 µL injection of the plasma extract in solvent 2 (no dilution) was used. Full scan MS acquisition (*m/z* 50 – 1000, 1 s/spectrum) was performed on a pooled sample. An extracted ion chromatogram on the precursor ion provided a retention time for the potential ion of interest. Several targeted MS/MS methods were created with every exact mass and its corresponding retention time. Purine and HP-921 were used as reference ions. These methods provided MS/MS spectra at 10, 20 and 40 V collision energy. The product ion scans were analyzed for the corresponding fragment used in the MRM method. If the precursor and product ion were found, then the identification of the analyte was investigated.

A

Time [min]	A [%]	B [%]	Flow [mL/min]	Max. Pressure Limit [bar]
0.00	100.0	0.0	0.350	400.00
4.50	100.0	0.0	0.350	---
12.50	85.0	15.0	0.350	---
18.00	82.0	18.0	0.350	---
30.00	30.0	70.0	0.350	---
45.00	23.0	77.0	0.350	---
47.00	2.0	98.0	0.350	---
51.00	2.0	98.0	0.350	---
53.00	100.0	0.0	0.350	---

B

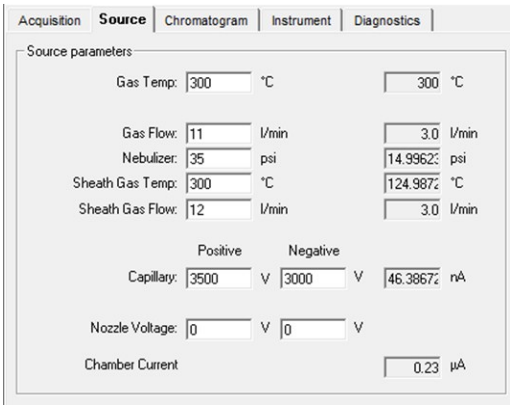

Figure S12 LC-AJS conditions for separation of unknown analytes using IPA/MeOH/water (5:1:4) with 5 mM ammonium acetate and 0.1 % acetic acid (Pump A), IPA/water (99:1) with 5 mM ammonium acetate and 0.1 % acetic acid (Pump B), and the gradient reported in (A). The source conditions are reported in (B).

3.2 LC-MS Data

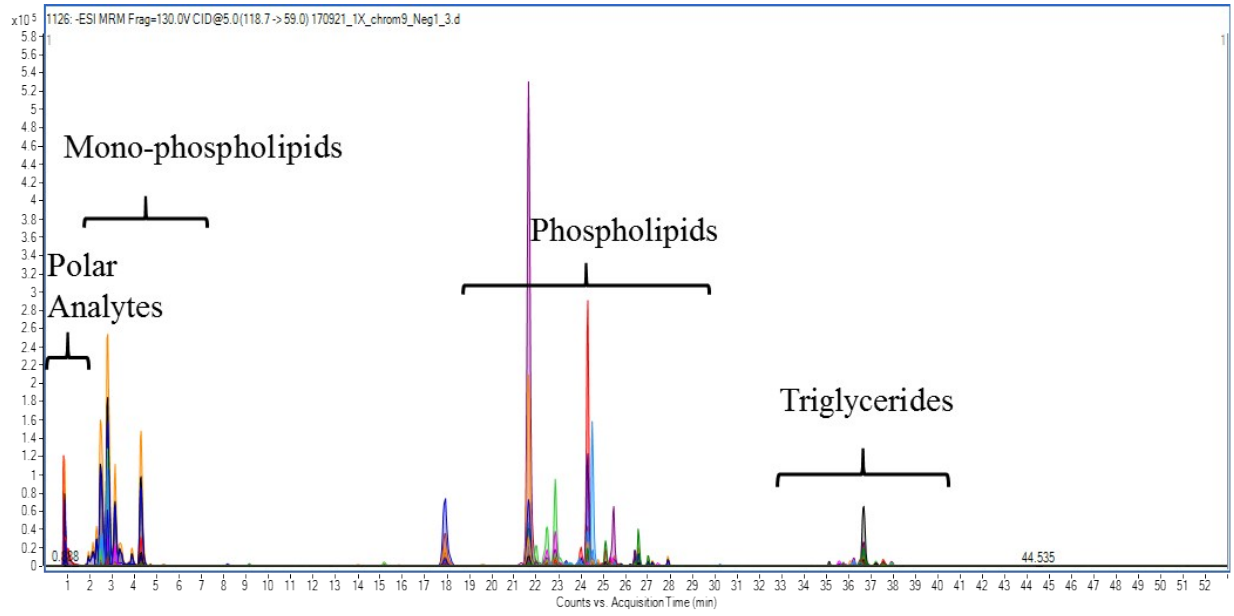

Figure S13 Zorbax C18, 150 x 2.1 mm, 1.8µ column was used with the method described in Figure S12. Data shown here were collected on a 6470 QQQ using the MRM parameters in the MRM-profiling study. Small polar analytes elute in the first minute followed by lyso-phospholipids, then phospholipids, and finally triacylglycerides.

Table S4 LC-MS identification results[a]

ID	Precursor Ion (*m/z*)	Product Ion (*m/z*)	Exact mass (*m/z*)	RT (min)	Adduct	F CAD	M CAD	PAD
No ID	60.9	43.9	Not found in LC method					↑
No ID	76	58	Not found in LC method			↑	↑	↑
Choline	104	45	104.1071	3	M+H			↑
No ID	114	43	114.0657	1	M+H			↑
Octylamine	130	71	130.1586	0.9	M+H	↑	↑	↑
	130	43	130.1586	0.9	M+H			
	130	56	130.1586	0.9	M+H			
	130	85	130.1586	0.9	M+H			
No ID	144.7	85	144.1017	1	M+H	↑		↑
Carnitine	161.9	85	162.1123	0.9	M+H	↑		↑
	162	103	162.1123	0.9	M+H			
	162	59	162.1123	0.9	M+H			
γ-hydroxy-L-homoarginine	204.9	85	205.1271	1	M+H	↑		↑
	204.9	86	205.1271	1	M+H			
No ID	218	85	218.1084	1	M+H			↑
No ID	229.1	142.1	229.1544	0.9	M+H	↑		↑
No ID	232	85	Not found in LC method			↑		↑
No ID	246.1	85	Not found in LC method					↑
No ID	286	85	Not found in LC method			↑		↑
No ID	288	85	Not found in LC method			↑		↑
	288.1	85.1						
	288.1	85						
No ID	316.1	85						↑
No ID	369.1	287.1	369.3511	37.5		↓		↓
	369.2	147.2	369.3511	37.5				
	369.2	119.2	369.3511	37.5				
	369.2	175.2	369.3511	37.5				
	369.2	109.2	369.3511	37.5				
	369.2	121.2	369.3511	37.5				
	369.2	91.2	369.3511	37.5				
	369.2	57.2	369.3511	37.5				
	369.2	193.2	369.3511	37.5				
	369.2	147	369.3511	37.5				
	369.2	85	369.3511	37.5				

	369.2	207.2	369.3511	37.5				
	369.3	41.3	369.3511	37.5				
	369.4	68.4	369.3511	37.5				
No ID	370.1	147	370.3546	37		↓	↓	↓
	370.1	288.1	370.3546	37				
	370.1	229.1	370.3546	37				
	370.2	69.2	370.3546	37				
	370.2	148.2	370.3546	37				
	370.2	176.2	370.3546	37				
	370.2	149.2	370.3546	37				
	370.2	120.2	370.3546	37				
	370.2	41.2	370.3546	37				
	370.2	122.2	370.3546	37				
	370.2	92.2	370.3546	37				
	370.2	194.2	370.3546	37				
	370.2	97	370.3546	37				
	370.3	97.1	370.3546	37				
	370.3	110.3	370.3546	37				
	370.3	93.1	370.3546	37				
MonoChain-PC	520.1	104	520.3371	2.6	M+H	↓	↓	
MonoChain-PC	521.2	104	521.3427	2.6	M+NH4	↓	↓	↓
MonoChain-PC	542	483	542.3215	2.5	M+H	↓	↓	
	542.1	104	542.3215	2.5	M+H			
No ID	632.3	264.3	Not found in LC method			↓		
20:5 Cholesteryl ester	671.3	303	671.5742	37.5	M+H	↓	↓	↓
SM(34:1)	725.2	542.2	725.5563	19.5	M+Na	↓	↓	
PC(34:2)	758.2	104	758.5691	22.9	M+H	↓	↓	
	758.4	86	758.5691	22.9	M+H			
	780.1	575.1	780.5515	22.9	M+Na	↓	↓	
	780.1	721.1	780.5515	22.9	M+Na			
	780.2	147	780.5515	22.9	M+Na			
	780.2	597.2	780.5515	22.9	M+Na			
	780.2	86	780.5515	22.9	M+Na			
SM(38:1)	759.2	184	759.6366	22.5	M+H	↓	↓	
	759.3	86	759.6366	22.5	M+H			
	781.2	147	781.6187	22.5	M+Na	↓	↓	
	781.2	598.2	781.6187	22.5	M+Na			
	781.2	576.2	781.6187	22.5	M+Na			
	781.2	86	781.6187	22.5	M+Na			

SM(40:2)	785.2	184	785.653	23.8	M+H	↓		
	807.2	624.2	806.5057	23.8	M+Na	↓	↓	
	807.3	147	806.5057	23.8	M+Na			
PC(36:2)	786.1	104	786.6005	25	M+H	↓		
	786.3	86	786.6005	25	M+H			
	808.2	625.2	808.5829	25	M+Na			
	808.2	603.2	808.5829	25	M+Na	↓	↓	
	808.3	147	808.5829	25	M+Na			
SM(40:1)	787.2	184	787.6692	25.1	M+H	↓		
	809.2	147	809.6509	25.1	M+Na	↓	↓	
	809.2	626.2	809.6509	25.1	M+Na			
PC(37:4)	796.1	737.1	796.5239	26.3	M+H	↓	↓	
	796.2	86	796.5239	26.3	M+H			
PC(38:6)	806.3	147	806.5662	23.6	M+H	↓	↓	
TAG	848.5	549.5	848.7687	37	M+NH4		↑	
TAG	850.4	577.2	850.7868	38	M+NH4			
	850.5	551.5	850.7868	38	M+NH4	↑	↑	
	850.5	577	850.7868	38	M+NH4			
TAG	851.2	577	851.7101	35.8	M+H		↑	
TAG	874.3	575.3	874.7828	37.3	M+NH4		↑	
	874.4	601.2	874.7828	37.3	M+NH4			
TAG	876.3	577.3	876.7995	38.5	M+NH4			
	876.4	603.2	876.7995	38.5	M+NH4	↑	↑	
	876.5	577	876.7995	38.5	M+NH4			
	876.5	603	876.7995	38.5	M+NH4			
TAG	877.3	578.3	877.803	38.6	M+H			
	877.4	604.2	877.803	38.6	M+H		↑	
	877.5	579	877.803	38.6	M+H			
TAG	878.3	577.3	878.7289	36.2	M+NH4		↑	
Salicylic acid	136.9	92.9	137.0252	1	M-H	↑	↑	↑
p-cresol sulfate	186.9	106.9	187.0064	9.6	M-H		↑	↑

a) If known, the exact mass, RT, adduct formed, and compound identification is listed. The up and down arrows in the female CAD, male CAD, and PAD columns indicate if the analyte was up or down regulated in the model.

Table S5 Library of Prec and NL scans for the discovery phase

Mode	Type	Value (amu for NL and *m/z* for Prec)	Functional Group
Negative	NL	27	H_20 - amines, aromatic nitrile, aminosulphonic acids[47]
Negative	NL	28	CO - carboxylic acids, adehydes, H_2CN - nitroaromatics[47]
Negative	NL	30	NO - nitroaromatics, CH2O - aldehydes[47]
Negative	NL	44	CO_2 - carboxylic acids, carbamates[47]
Negative	NL	46	NO_2 - nitroaromatics, CH_2O_2 - carboxylic acids[47]
Negative	NL	62	H_2O and CO_2 [37]
Negative	NL	64	SO_2 - sulfonic acids, sulfonates[47]
Negative	NL	76	Phosphatidylglycerol (PG)[40]
Negative	NL	80	SO_3 - sulfonic acids[47]
Negative	NL	87	Phosphatydylserine (PS) head group[44]
Negative	NL	98	Steroid conjugate [37]
Negative	NL	121	$C_3H_7NO_2S$ - cysteine conjugates[47]
Negative	NL	146	$C_6H_{10}O_4$ - deoxyhexoside[47]
Negative	NL	153	Phosphoglycerols including phosphatidic acids (PA) and Lysophosphatidylglycerol (LysoPG) [44]
Negative	NL	164	$C_6H_{12}O_5$ - rhamnoside[47]
Negative	NL	176	$C_6H_8O_6$ – glucoronides// steroid conjugate[37, 47]
Negative	NL	194	Steroid conjugate[37]
Negative	NL	203	$C_8H_{13}NO_5$ - conjugate with N-acetylglucosamine (benzylic) [47]
Negative	NL	250	$C_8H_{14}N_2O_5S$ - conjugate with gamma-GluCys[47]
Negative	NL	282	Oleic acid; Phosphatidylinositol (PI) [44]
Negative	NL	355	Phosphatidylcholine (PC), alkelnyl-acyl PC (ePC), sphingomyelin (SM) and LysoPC[4]
Negative	NL	444	Oleic acid and inositol; PI[44]
Negative	Prec	59	Arachinonic acid (fatty acid) [37]
Negative	Prec	80	SO_3^{-}[37]
Negative	Prec	97	Sulfatide (ST)// HSO_4^{-}[4, 37, 40]
Negative	Prec	115	HETE[37]
Negative	Prec	127	HETE[37]
Negative	Prec	135	PA
Negative	Prec	140	Phosphatidylethanolamine (PE)
Negative	Prec	145	HETE[37]
Negative	Prec	151	Leukotrienes[37]
Negative	Prec	153.1	glycerophosphate[4, 43]
Negative	Prec	155	HETE[37]
Negative	Prec	167	HETE[37]
Negative	Prec	168	SM; demethylated headgroup[44]
Negative	Prec	171	PG

Negative	Prec	175	HETE[37]
Negative	Prec	179	HETE[37]
Negative	Prec	191	Glucuronide[37]
Negative	Prec	193	Glucuronide[37]
Negative	Prec	195	Leukotrienes[37]
Negative	Prec	196	PE; dilyso-H_2O[44]
Negative	Prec	199	glycerolipids; Dodecanoic acid residue
Negative	Prec	207	HETE[37]
Negative	Prec	219	HETE[37]
Negative	Prec	223	PI
Negative	Prec	225.2	glycerolipids; myristoleic acid residue and Sulfoquinovosyldiacylglycerol
Negative	Prec	226	prostaglandin[37]
Negative	Prec	227.2	glycerolipids; Myristicacid residue
Negative	Prec	241	PI head group, nositol phosphate[38, 40]
Negative	Prec	253.2	glycerolipids; Palmitoleic/Sapienic acid residue
Negative	Prec	255.2	glycerolipids; Palmitic acid residue
Negative	Prec	275.2	glycerolipids; stearidonic acid
Negative	Prec	277.2	glycerolipids; gama-Linolenic acid residue
Negative	Prec	279.2	Glycosylphosphatidylinositol (GPI) 18:243, 44
Negative	Prec	281.2	GPI 18:143, 44
Negative	Prec	283.2	GPI 18:3[43, 44]
Negative	Prec	301	glycerolipids; Eicosapentaenoic acid residue
Negative	Prec	305.2	glycerolipids; eicosatrienoic residue
Negative	Prec	307.3	glycerolipids; eicosadienoic residue
Negative	Prec	309.3	glycerolipids; Gondoic acid residue
Negative	Prec	311.3	glycerolipids; Arachidicacid residue
Negative	Prec	327.3	glycerolipids; docosahexaenoic DHA residue
Negative	Prec	329.3	glycerolipids; Eicosapentaenoic acid EPA residue
Negative	Prec	331.3	glycerolipids; Docosatetraenoic acid residue
Negative	Prec	333	Leukotrienes[37]
Negative	Prec	335.2	glycerolipids; docosadienoic residue
Negative	Prec	337.3	glycerolipids; Erucic acid residue
Negative	Prec	339.3	glycerolipids; Behenic acid residue
Negative	Prec	355.3	glycerolipids; nisinic acid residue
Negative	Prec	365.4	glycerolipids; nervonic acid residue
Negative	Prec	367.4	glycerolipids; Lignoceric acid residue
Negative	Prec	395.4	glycerolipids; cerotic acid residue
Negative	Prec	423.4	glycerolipids; melissics acid residue
Negative	Prec	451.4	glycerolipids; lacceroic acid residue
Negative	Prec	479.5	glycerolipids; geddicacid residue
Negative	Prec	507.5	glycerolipids; montanic acid residue

Positive	NL	17	NH_3- aliphatic amines (aromatic amines), oximes[47]
Positive	NL	18	H_2O - carboxylic acids, adehydes, ester[47]
Positive	NL	27	H_20 - amines, aromatic nitrile, aminosulphonic acids[47]
Positive	NL	28	CO - carboxylic acids, aldehydes, H_2CN - nitroaromatics[47]
Positive	NL	30	NO - nitroaromatics, CH_2O - aldehydes[47]
Positive	NL	32	CH4O - methyl esters[47]
Positive	NL	34.0	H_2S - thiols[47]
Positive	NL	36.0	HCl –chlorides and 2(H_2O) [41, 47]
Positive	NL	44.0	CO_2 - carboxylic acids, carbamates[47]
Positive	NL	46.0	NO_2 - nitroaromatics, CH_2O_2 - carboxylic acids[47]
Positive	NL	48	H_2O and HCHO- sphingosine[41]
Positive	NL	50	Chloromethane- PC[43]
Positive	NL	59.0	Choline species; $(CH_3)_3N$[40]
Positive	NL	64.0	CH_4OS - methionine sulfoxide[47]
Positive	NL	71.0	C_3H_5NO - serine residue[47]
Positive	NL	74.0	C_3H_6S - methionine side chain[47]
Positive	NL	80.0	SO_3 - sulfonic acids, HPO_3 - phosphates[47]
Positive	NL	81.0	HSO_3 - sulfonic acids[47]
Positive	NL	82.0	H_2SO_3 - sulfonate group[47]
Positive	NL	87	Serine; PS[43]
Positive	NL	98.0	H_3PO_4 - phosphates[47]
Positive	NL	103	Lysophospholipid[37]
Positive	NL	115	Phosphatidic acid
Positive	NL	121	$C_3H_7NO_2S$ - cysteine conjugates[47]
Positive	NL	128	HI - aromatic iodides[47]
Positive	NL	130	$C_6H_{10}O_3$ - dideoxyhexoside[47]
Positive	NL	132	$C_5H_8O_4$ - pentoside[47]
Positive	NL	141	PE head group[40, 44]
Positive	NL	146	Pro/anthocyanidins; $C_6H_{10}O_4$ - deoxyhexoside, $C_5H_{10}N_2O_3$ - conjugate with gamma-GluCys or gluthatione[47, 48]
Positive	NL	162	Pro/anthocyanidins; $C_6H_{10}O_5$ - hexoside[47, 48]
Positive	NL	163	$C_5H_9NO_3S$ - N-acetylcysteine conjugate[47]
Positive	NL	176	$C_6H_8O_6$ - glucuronides[47]
Positive	NL	179	Glycosylinositolphosphoceramide (GIPC)
Positive	NL	183	Phosphocholine (Li+)[43]
Positive	NL	185	PS head group[40, 44]
Positive	NL	189	PG headgroup[49]
Positive	NL	194	$C_6H_{10}O_7$ - glucuronides (benzylic) [47]
Positive	NL	203	$C_8H_{13}NO_5$ - conjugate with N-acetylglucosamine (benzylic) [47]
Positive	NL	205	lysophospholipids[37]
Positive	NL	217	glycerolipids; Dodecanoic acid residue[39]
Positive	NL	221	$C_8H_{15}NO_6$ - conjugate with N-acetylglucosamine[47]

Positive	NL	228	TAG 14:0
Positive	NL	245	glycerolipids; Myristicacid residue[39]
Positive	NL	248	$C_9H_{12}O_8$ – malonylglucuronides[47]
Positive	NL	250	$C_8H_{14}N_2O_5S$ - conjugate with gamma-GluCys[47]
Positive	NL	254	TAG 16:1[43]
Positive	NL	256	TAG 16:0[43]
Positive	NL	257	glycerolipids; myristoleic acid residue[39]
Positive	NL	260	glycerophosphoserine[37]
Positive	NL	266	$C_9H_{14}O_9$ - malonylglucoronides (benzylic) [47]
Positive	NL	271	glycerolipids; Palmitoleic/Sapienic acid residue TAG[38, 39]
Positive	NL	273	TAG 16:0[38, 39]
Positive	NL	273.2	TAGs; NH_4^+ $CH_3(CH_2)_{14}COOH$[38]
Positive	NL	277	PI[49]
Positive	NL	277.2	TAGS[38]
Positive	NL	278	TAG 18:3[43]
Positive	NL	280	TAG 18:2[43]
Positive	NL	282	TAG 18:1[43]
Positive	NL	284	TAG 18:0[43]
Positive	NL	293	glycerolipids; stearidonic acid
Positive	NL	295	TAG[39]
Positive	NL	297	TAG[39]
Positive	NL	299	TAG[38, 39]
Positive	NL	301	TAG[38]
Positive	NL	304	TAG 20:4[43]
Positive	NL	307	$C_{10}H_{17}N_3O_6S$glutathione conjugates[47]
Positive	NL	312	TAG 20:0[43]
Positive	NL	319	glycerolipids; Eicosapentaenoic acid residue[39]
Positive	NL	321	glycerolipids; Arachidonic acid residue[39]
Positive	NL	323.0	glycerolipids; eicosatrienoic residue[39]
Positive	NL	325.0	TAG 20:2[39]
Positive	NL	327.0	TAG 20:1[39]
Positive	NL	328	TAG 22:0[43]
Positive	NL	329.0	TAG 20:0[39]
Positive	NL	341.0	Digalactosyldiacylglycerol (DGDG) and monogalactosyldiacylglycerol (MGDG)[50]
Positive	NL	345.0	glycerolipids; docosahexaenoic DHA residue[39]
Positive	NL	347.0	glycerolipids; Eicosapentaenoic acid EPA residue[39]
Positive	NL	349.0	glycerolipids; Docosatetraenoic acid residue[39]
Positive	NL	353.0	glycerolipids; docosadienoic residue[39]
Positive	NL	355.0	glycerolipids; Erucic acid residue[39]

Positive	NL	357.0	glycerolipids; Behenic acid residue[39]
Positive	NL	375.0	glycerolipids; nisinic acid residue
Positive	NL	383.0	glycerolipids; nervonic acid residue
Positive	NL	385.0	glycerolipids; Lignoceric acid residue[39]
Positive	NL	413.0	glycerolipids; cerotic acid residue
Positive	NL	441.0	glycerolipids; melissics acid residue
Positive	NL	469.0	glycerolipids; melissics acid residue
Positive	NL	497.0	glycerolipids; melissics acid residue
Positive	NL	525.0	glycerolipids; melissics acid residue
Positive	Prec	85	Acylcarnitines[4]
Positive	Prec	86	PC, LPC, SM; $OHCH_2CH_2NMe_3$-H_2O[40]
Positive	Prec	104	PC, LPC, SM; choline[40]
Positive	Prec	147	Lysophospholipids[37]
Positive	Prec	153	Glycerophosphate[43]
Positive	Prec	166	PC/LPC/SM [40]
Positive	Prec	181	Lysophospholipids[37]
Positive	Prec	184	Phosphatidylcholine (PC), alkelnyl-acyl PC (ePC), sphingomyelin (SM) and LysoPC[40, 44]
Positive	Prec	256.3	Ceramides 16:0[42]
Positive	Prec	262.3	Ceramides d18:2[42]
Positive	Prec	264	Ceramides[37]
Positive	Prec	264.3	Ceramides (d18:1; sphingosines)/Cerebrosides[42, 46]
Positive	Prec	266	Ceramides[37]
Positive	Prec	266.4	Ceramides (d18:0; sphinganines) [42, 46]
Positive	Prec	279	Ceramides[43]
Positive	Prec	280	Ceramides[37]
Positive	Prec	282.2	Ceramides (t18:0 4-hydroxysphinganines) [42, 46]
Positive	Prec	282.4	Ceramides 18:0[37, 42]
Positive	Prec	283	Ceramides[43]
Positive	Prec	284.3	Ceramides 18:0[42]
Positive	Prec	292.3	Ceramides d20:1[42]
Positive	Prec	292.4	Ceramides (d20:1)[46]
Positive	Prec	300.3	Ceramides 18:0(OH) [42]
Positive	Prec	301	Pro/anthocyanidins[48]
Positive	Prec	303	Pro/anthocyanidins[48]
Positive	Prec	307.3	Ceramides [42]
Positive	Prec	310.3	Ceramides 20:0[42]
Positive	Prec	312	Pro/anthocyanidins[48]
Positive	Prec	328.3	Ceramides 20:0(OH) [42]
Positive	Prec	338.3	Ceramides 22:0[42]
Positive	Prec	340.4	Ceramides 22:0(OH) [42]
Positive	Prec	352.4	Ceramides 23:1[42]

Positive	Prec	354.4	Ceramides 23:0[42]
Positive	Prec	356.4	Ceramides 23:0(OH) [42]
Positive	Prec	366.4	Ceramides 24:1[42]
Positive	Prec	368.4	Ceramides 24:0 or 23:1(OH) [42]
Positive	Prec	369.1	Cholesterol esters[51]
Positive	Prec	370.4	Ceramides 23:0(OH) [42]
Positive	Prec	380.4	Ceramides 25:1[42]
Positive	Prec	382.4	Ceramides 25:0 or 24:1(OH) [42]
Positive	Prec	384.4	Ceramides 24:0[42]
Positive	Prec	523	TAG, NH_4 fatty acyl substituent[38]
Positive	Prec	537	TAG, NH_4 fatty acyl substituent[38]
Positive	Prec	549.5	TAG, NH_4 fatty acyl substituent[38]
Positive	Prec	551.5	TAG, NH_4 fatty acyl substituent[38]
Positive	Prec	563.5	TAG, NH_4 fatty acyl substituent[38]
Positive	Prec	565.5	TAG, NH_4 fatty acyl substituent[38]
Positive	Prec	577	TAG, NH_4 fatty acyl substituent[38]
Positive	Prec	579	TAG, NH_4 fatty acyl substituent[38]
Positive	Prec	603	TAG[38]